
# Effects of Karlovitz number on super-adiabatic temperature and burning rate in lean hydrogen-air turbulent flames

# Effects of Karlovitz number on super-adiabatic temperature and burning rate in lean hydrogen-air turbulent flames

Xuefeng Guan,[1,2,3] Hsu Chew Lee,[1] Peng Dai,[1,a)] Minping Wan,[1,2,3] and Andrei N. Lipatnikov[4]

[1)] *Guangdong Provincial Key Laboratory of Turbulence Research and Applications, Department of Mechanics and Aerospace Engineering, Southern University of Science and Technology, Shenzhen, 518055, China*

[2)] *Guangdong-Hong Kong-Macao Joint Laboratory for Data-Driven Fluid Mechanics and Engineering Applications, Southern University of Science and Technology, Shenzhen, 518055, China*

[3)] *Shenzhen Key Laboratory of Complex Aerospace Flows, Department of Mechanics and Aerospace Engineering, Southern University of Science and Technology, Shenzhen, 518055, China*

[4)] *Department of Mechanics and Maritime Sciences, Chalmers University of Technology, Göteborg, 412 96, Sweden*

(Dated: 22 April 2026)

Analyzed in the paper are previously published and newly generated three-dimensional direct numerical simulation data obtained from statistically planar and one-dimensional, lean complex-chemistry $H_2$-air flames propagating in a box with forced turbulence. Under the study conditions, root-mean-square turbulent velocity is varied from 2.2 to 54 laminar flame speeds $S_L$, integral length scale of turbulence is varied from 0.5 to 2.25 laminar flame thicknesses, Damköhler and Karlovitz numbers are varied from 0.01 to 0.53 and from 10 to 1315, respectively. Two equivalence ratios, 0.5 and 0.35, are explored. Turbulent burning velocities are evaluated not only for these eight low Lewis number flames, but also for equidiffusive counterparts to them. Analyses of these burning velocities and conditioned profiles of temperature, fuel consumption and heat release rates show significant influence of differential diffusion effects on the local structure of flame reaction zones and burning rate in all eight cases, even at Karlovitz number $Ka$ as high as 1315. On the contrary, both magnitude of super-adiabatic temperature and probability of finding it are decreased with increasing $Ka$. The latter trend is attributed to intensification of turbulent mixing in flame oxidation zones where fuel consumption rate is low. Therefore, the two phenomena (increase in burning rate due to differential diffusion effects and appearance of super-adiabatic hot spots) are not inextricably linked. Differential diffusion effects can increase burning rate even if turbulence is intense enough to erase super-adiabatic hot spots.

[a)]Electronic mail: daip@sustech.edu.cn

## I. INTRODUCTION

As reviewed elsewhere,[1–4] turbulent burning of lean $H_2$-containing mixtures is greatly affected by differences between molecular diffusion coefficients of hydrogen, oxygen, and heat. Henceforth, a single abbreviation DDE means differential diffusion effects and subsumes both diffusional-thermal effects,[5] which stem from differences in molecular diffusivities of $H_2$ and heat, and preferential diffusion effects,[6] which stem from differences in molecular diffusivities of fuel and oxidant. On the global level, such effects manifest themselves in abnormally high ratios $U_T/S_L$ of turbulent and laminar burning velocities, found in pioneering measurements by Karpov et al.[7,8] and in many subsequent experiments, e.g., see review articles[2,3] and recent papers.[9–16] On the local level, DDE manifest themselves in significant variations in the equivalence ratio $\phi$, species mass fractions $Y_k$, and temperature $T$, including appearance of hot spots characterized by super-adiabatic temperatures $T > T_{ad}$. Such local phenomena were recently explored in complex-chemistry Direct Numerical Simulation (DNS) studies[17–34] and experiments.[35,36] These global and local phenomena are commonly attributed[1–4,37,38] to imbalance of molecular fluxes of heat and chemical energy from and to, respectively, inherently laminar thin reaction zones stretched by turbulent eddies. This imbalance is greatly affected by the local flame curvature and strain rate.[2–4,17,20,22–24,26,27,31,33]

However, interplay of these phenomena and a range of conditions associated with importance of them are still unclear. On the one hand, both DNS[18,19,21,28,30] and experimental[36] data indicate reduction of local variations in $\phi$ or/and disappearance of super-adiabatic temperatures with increasing normalized rms velocity $u'/S_L$ or/and Karlovitz number $Ka \propto (u'/S_L)^{3/2}(L/\delta_L)^{-1/2}$. Here, $L$ is an integral length scale of turbulence and $\delta_L$ is laminar flame thickness. Such local trends are often associated with mitigation of other DDE by turbulence. For instance, a decrease in "the percentage of $U_T$, which is attributed to superadiabatic burning" was recently considered to quantify "the decrease of differential diffusion effects at high Karlovitz numbers,"[30] see pp. 5-6 in the cited paper. On the other hand, the present authors are not aware on any experimental study that shows reduction of the influence of DDE on $U_T/S_L$ with increasing $u'/S_L$ or/and $Ka$. Abnormally large ratios of $U_T/S_L$ were well documented in experiments at extremely high[7,8,11] $Ka \gg 1$ or at smaller but still very large[12,16] $Ka = O(10^3)$. These data imply that even very intense turbulence does not suppress DDE on the global level.

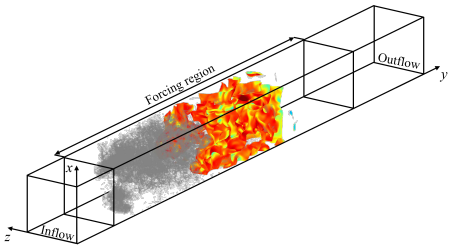


FIG. 1. Typical flame image. Iso-surfaces of vorticity magnitude equal to 300 $\mathrm{ms}^{-1}$ and combustion progress variable equal to 0.86 are shown in gray and other colors, respectively. The color scale characterizes the local fuel consumption rate. Case $\mathrm{C_{Ka}}$.

The emphasized dichotomy, i.e., survival of DDE on the global level (abnormally high $U_T/S_L$ in lean $H_2$-containing mixtures even at $Ka \gg 1$) and disappearance of them on the local level[18,19,21,28,30,36] calls for a target-directed study. The present work aims to clarify this dichotomy. For this purpose, the influence of turbulence and DDE on both burning rate and super-adiabatic temperature is further explored by analyzing DNS data obtained from lean $H_2$-air flames in a wide range of Karlovitz numbers.

## II. DNS DATA

Since most of the DNS data analyzed in the following were already reported,[39–47] let's restrict ourselves to a summary of the major DNS attributes and refer the interested reader to the cited articles.

This study deals with statistically planar and one-dimensional, adiabatic, lean (the equivalence ratio $\phi = 0.35$ or 0.5) $H_2$-air, complex-chemistry flames propagating along $y$-direction in a box of $\Lambda \times M\Lambda \times \Lambda$ with forced turbulence. Numerical meshes are uniform and consist of $N \times MN \times N$ cells. The box widths $\Lambda$ and the numbers $M$ and $N$ are reported in Table I. Flame configuration is illustrated in Fig. 1.

The flames are simulated using software DINO[48] to solve unsteady, three-dimensional reacting flow equations in the limit of a low Mach number. The ideal gas state equation, a chemical mechanism (22 reversible reactions between 9 species) by Kéromnès et al.,[49] and mixture-averaged molecular transport model[50] are also invoked. It is worth noting that

contemporary numerical studies of stable laminar flames routinely use the multi-component transport model with Soret effect, e.g., to improve predictions of $S_L$. Such advanced transport models were also adopted in a few DNS studies of unstable laminar[51] or turbulent[30] combustion of lean $H_2$-air mixtures. While results of these studies do show quantitative effects such as enhancement of laminar flame instabilities[51] or an increase in turbulent burning rate[30] due to Soret diffusion, "qualitative observations and trends" are not changed.[30] Accordingly, the mixture-averaged transport model without Soret effect is still widely used for numerical research into turbulent flames in order to make three-dimensional DNS of turbulent combustion affordable. For instance, most DNS results reviewed recently[52] were obtained adopting this simplified approach. Since the focus of the present work is placed on qualitative trends such as the influence of an increase in $Ka$ on appearance of super-adiabatic hot spots, the same simplified, but still state-of-the-art approach is adopted here.

Inflow and outflow boundary conditions are set along the streamwise direction $y$. Other boundary conditions are periodic. Turbulence is generated by adopting variable-density linear forcing method.[53,54] Note that comparison of DNS results obtained from the forced turbulence and decaying turbulence (i.e., when the linear forcing method was switched off) did not reveal substantial differences between manifestations of DDE in both cases.[39]

Combustion simulations were started by embedding a planar laminar flame (computed using Cantera[50]) in the center of the computational domain at $t = 0$.

Major characteristics of the studied flames are reported in Table I. Here, $L = u'^3/\varepsilon_0$ is target value of an integral length scale; $\varepsilon_0 = 2\nu\langle S_{ij}S_{ij}\rangle$ is dissipation rate averaged over forced turbulence volume before embedding a flame; $S_{ij} = (\partial u_i/\partial x_j + \partial u_j/\partial x_i)/2$ is the rate-of-strain tensor; $\nu$ is kinematic viscosity of fresh gas; and the summation convention applies to repeated indexes. The speed $S_L$, thickness $\delta_L = (T_b - T_u)/\max|\nabla T|$, time scale $\tau_F = \delta_L/S_L$, and Lewis number $Le = \alpha_u/D_{H_2,u}$ are computed using chemical mechanism by Kéromnès et al.[49] and Cantera[50] under room conditions. Here, $\alpha_u$ and $D_{H_2,u}$ are molecular heat diffusivity of a mixture and mass diffusivity of $H_2$ in the mixture, respectively; and subscript $u$ or $b$ refers to unburned or burned gas, respectively. The Reynolds number $Re_\lambda = u'\lambda/\nu$, Damköhler number $Da = \tau_t/\tau_F$, and Karlovitz number $Ka = \tau_F/\tau_K$ are evaluated using Taylor microscale $\lambda = (10\nu_u u'/\varepsilon_{le})^{1/2}$, integral time scale $\tau_t = L/u'$, and Kolmogorov time scale $\tau_K = (\nu_u/\varepsilon_{le})^{1/2}$. To characterize the turbulence that the flame meets and that affects the flame leading edge (where DDE are most pronounced, as will

TABLE I. Major characteristics of simulated lean hydrogen-air flames under room conditions.

| Case | $\phi$ | $S_L$,m/s | $\delta_L$,mm | $Le$ | $\frac{u'}{S_L}$ | $\frac{L}{\delta_L}$ | $Da$ | $Ka$ | $Re_\lambda$ | $\frac{\Delta x}{\eta}$ | $N$ | $M$ | $\Lambda$,mm | $\frac{\overline{U}_T}{S_L}$ | Ref. |
|---|---|---|---|---|---|---|---|---|---|---|---|---|---|---|---|
| A | 0.5 | 0.58 | 0.41 | 0.39 | 2.2 | 1.1 | 0.53 | 9.9 | 21 | 1.08 | 64 | 18 | 2.4 | 4.1 | [39] |
| B | 0.5 | 0.58 | 0.41 | 0.39 | 4.0 | 1.1 | 0.29 | 26 | 26 | 1.13 | 96 | 18 | 2.4 | 5.4 | [39] |
| C | 0.5 | 0.58 | 0.41 | 0.39 | 11.2 | 1.1 | 0.10 | 121 | 44 | 1.85 | 128 | 16 | 2.4 | 8.2 | [39] |
| $C_{Da}$ | 0.5 | 0.58 | 0.41 | 0.39 | 22.4 | 2.2 | 0.10 | 246 | 92 | 1.75 | 384 | 7 | 4.8 | 17.0 | new |
| $C1_{Da}$ | 0.36 | 0.33 | 0.41 | 1.0 | 22.4 | 2.2 | 0.10 | 154 | 86 | 1.37 | 320 | 10 | 4.8 | 5.2 | new |
| $C_{Ka}$ | 0.5 | 0.58 | 0.41 | 0.39 | 14.2 | 2.2 | 0.14 | 128 | 71 | 1.24 | 320 | 10 | 4.8 | 20.6 | new |
| $C1_{Ka}$ | 0.36 | 0.33 | 0.41 | 1.0 | 14.2 | 2.2 | 0.14 | 80 | 61 | 0.97 | 320 | 10 | 4.8 | 5.7 | new |
| D | 0.35 | 0.12 | 0.92 | 0.36 | 54.1 | 0.5 | 0.01 | 1315 | 44 | 1.85 | 128 | 16 | 2.4 | 14.9 | [42] |
| E | 0.35 | 0.12 | 0.92 | 0.36 | 11.2 | 0.5 | 0.04 | 125 | 20 | 1.13 | 64 | 16 | 2.4 | 12.1 | [42] |
| F | 0.35 | 0.12 | 0.92 | 0.36 | 11.2 | 1.2 | 0.10 | 85.7 | 29 | 1.07 | 128 | 16 | 5.6 | 23.9 | [42] |

be discussed later), Karlovitz numbers are evaluated using the dissipation rate $\varepsilon_{le}$ averaged over the flame-brush leading zone, i.e., the zone where the transverse-averaged combustion progress variable $0.01 < \overline{c}_F(y,t) < 0.05$. Here, $c_F = 1 - Y_F/Y_{F,u}$ and $Y_F$ designates fuel mass fraction. Finally, $\eta_K = (\nu^3/\varepsilon_{le})^{1/4}$ is Kolmogorov length scale in the leading zone and $\Delta x$ is grid spacing. The reader interested in further details is referred to the papers cited at the beginning of this section.

In Table I, case names used in the original papers cited in the rightest column are retained. Two new cases, $C_{Da}$ and $C_{Ka}$, have been designed (i) starting from case C, (ii) increasing the domain width $\Lambda$ and length scale $L$, but (iii) retaining roughly the same $Da$ and $Ka$, respectively. These two cases were newly designed to compare the influence of Damköhler and Karlovitz numbers on major characteristics of premixed turbulent flames C, $C_{Da}$, and $C_{Ka}$. However, since this original task is beyond the scope of the present analysis, results of such a comparative study will be presented in a future paper. Here, these two cases are included to expand the ranges of $Ka$ and $L/\delta_L$ studied. Two other new cases $C1_{Da}$ and $C1_{Ka}$ are equidiffusive counterparts of cases $C_{Da}$ and $C_{Ka}$, respectively. These two pairs of cases ($C_{Da}$ and $C1_{Da}$ or $C_{Ka}$ and $C1_{Ka}$) have been designed to target-directly explore DDE, with other major things being equal. For this purpose, in each equidiffusive case $C1_{Da}$ or $C1_{Ka}$, (i) diffusivities of all species are set equal to molecular heat diffusivity of the mixture, (ii)

the equivalence ratio is decreased to increase $\delta_L$ and, hence, to retain the same $L/\delta_L$ (recall that the length scale $L$ is proportional to the computational domain width $\Lambda$), and (iii) $u'$ is adjusted to retain the same $u'/S_L$. As a result, in both pairs of the new cases ($\mathrm{C_{Ka}}$ and $\mathrm{C1_{Ka}}$ or $\mathrm{C_{Da}}$ and $\mathrm{C1_{Da}}$), time-averaged normalized turbulent burning velocity $\overline{U}_T/S_L$, which is reported in the next-to-right column in Table I and will be discussed later, is significantly larger at a low $Le$, with $u'/S_L$, $L/\delta_L$, $Da$, or $Ka$ being the same. For comparison, in our previous simulations,[42] the equidiffusive counterparts A1-F1 to flames A-F were designed by solely setting diffusivities of all species equal to molecular heat diffusivity of the mixture, with all other things being equal. Accordingly, those six equidiffusive flames are characterized by a smaller $u'/S_L$ when compared to their low $Le$ counterparts.

Thus, there are two groups of low Lewis number flames. One group involves five lean ($\phi$=0.5) flames A, B, C, $\mathrm{C_{Da}}$, and $\mathrm{C_{Ka}}$, characterized by different Karlovitz numbers, which are increased from case A to case $\mathrm{C_{Da}}$. In three cases A-C, the increase in $Ka$ results solely from increasing $u'/S_L$, whereas the normalized length scale $L/\delta_L$ retains the same value. In case $\mathrm{C_{Da}}$ or $\mathrm{C_{Ka}}$, not only $u'/S_L$, but also $L/\delta_L$ are larger when compared to case C.

Another group involves three leaner ($\phi$=0.35) flames D, E, and F, characterized by different $Ka$, which is decreased from case D to case F. Originally, case D complemented case C and was designed to explore the influence of equivalence ratio on combustion in the same turbulent flow. Since this decrease in $\phi$ resulted in significantly increasing $u'/S_L$ and $Ka$, case E further complemented case C and was designed to study the influence of the equivalence ratio on combustion at the same non-dimensional $u'/S_L$ and the same dimensional length scale $L$. The third case F further complemented case C and was designed to investigate the influence of the equivalence ratio on combustion at the same $u'/S_L$ and the same non-dimensional $L/\delta_L$. In addition, cases (i) D and E, (ii) E and F, or (iii) D-F offer the opportunity to explore the influence of (i) $u'/S_L$, (ii) $L/\delta_L$, and (iii) $Ka$, respectively, on turbulent burning of the same mixture.

Reported in the next-to-right column in Table I are the mean normalized burning velocities evaluated by spatially integrating the mass Fuel Consumption Rate (FCR) $\dot{\omega}_F(\mathbf{x},t)$, i.e.,

$$U_T(t) = \frac{W_F}{\rho_u Y_{F,u} \Lambda^2} \iiint \dot{\omega}_F(\mathbf{x},t)\, d\mathbf{x}, \tag{1}$$

followed by time-averaging. Here, $\rho$ is the density and $W_F$ is fuel molecular weight.

TABLE II. Ratios of normalized turbulent burning velocities in low Le and equidiffusive flames.

| Pairs of cases | A | B | C | $C_{Da}$ | $C_{Ka}$ | D | E | F |
|---|---|---|---|---|---|---|---|---|
| Ratios | 1.43 | 1.64 | 1.91 | 3.16 | 3.27 | 4.38 | 5.73 | 4.98 |

For flames A-F and their equidiffusive counterparts, these results are discussed in detail elsewhere.[39,42]

For completeness, Table II reports ratios of normalized turbulent burning velocities $\overline{U}_T/S_L$ for eight pairs of low $Le$ and equidiffusive flames (for six pairs from A to F, these ratios are taken from earlier papers[39,42]). In all cases studied, $\overline{U}_T/S_L$ is significantly higher at $Le < 1$. For instance, $\overline{U}_T/S_L$ is equal to 14.9 and 3.4 in case D and its equidiffusive counterpart D1, respectively. Moreover, even dimensional $\overline{U}_T$ is larger by a factor of 1.6 in case D when compared to case D1, despite $S_L$=0.30 m/s is larger by a factor of 2.5 in the latter (equidiffusive) flame. Thus, an increase in $Le$ from 0.36 to 1.0 results in significantly increasing $S_L$, but decreasing $\overline{U}_T$ in the same turbulent flow. Since numerous experimental and numerical data indicate an increase in turbulent burning velocity not only by $S_L$, but also[16,37,55–59] by $L/\delta_L$, the emphasized increase in $\overline{U}_T$ with decreasing $Le$ cannot be explained by differences in the sole remaining (in addition to $S_L$ and $Le$) mixture characteristic, i.e., $\delta_L$, which is smaller in case D1. All these points considered together, i.e., an increase in $Le$ results in (i) increasing $S_L$, (ii) increasing $L/\delta_L$, but (iii) decreasing $\overline{U}_T$ in the same turbulent flow, can naturally be attributed to DDE. The present authors are not aware of an alternative model that is consistent with all three points (i)-(iii). Other (new) results that indicate importance of DDE in the studied low $Le$ flames will be discussed in the next section. Thus, DDE result in significantly increasing turbulent burning velocity even at $Ka$ as high as 1315 (case D) in line with classical[7,8] and recent[11,12,16] experimental data.

The following discussion is based on analyses of the conditioned profiles $\langle T|c_F\rangle(c_F)$, $\langle\dot{\omega}_F|c_F\rangle(c_F)$, and $\langle\dot{\omega}_T|c_T\rangle(c_T)$ of temperature, FCR, and Heat Release Rate (HRR), respectively. Methods adopted to sample such time-averaged conditioned profiles are described in detail elsewhere.[22] Moreover, the peak values of $T(\mathbf{x},t)$ are also sampled from the entire flame brushes at each instant and are averaged over time. Finally, probabilities of $T(\mathbf{x},t) > T_{ad}$ are evaluated for each bin of $c_F(\mathbf{x},t)$ by counting points characterized by $T(\mathbf{x},t) > T_{ad}$.

## III. RESULTS AND DISCUSSION

Fig. 2 shows conditioned profiles of (a)-(b) FCR or (c)-(d) HRR, sampled from the entire flame brush and averaged over time. The profiles are reported at $c_F > 0.4$, because the focus of the present study is placed on phenomena localized to large $c_F$. To stress the high magnitude of DDE in these low $Le$ mixtures, each profile is normalized using values of the plotted rate, obtained from the unstretched laminar flame at the same $\phi$ and the same $c_F$. Note that such profiles obtained from all equidiffusive flames addressed here are reduced to the same horizontal line $y = 1$.

In all low $Le$ cases, the normalized FCR and HRR are larger than unity (with the exception of a zone of $c_F > 0.9$ at $\phi = 0.5$, where the dimensional rates are very low) and are significantly increased with decreasing $c_F$. The computed large magnitudes of FCR and HRR in turbulent flames when compared to unstretched laminar flames are attributed to DDE. They are not further discussed here, because such effects are explored in detail in earlier papers,[22,42,44] where the DNS data obtained in cases A-E are analyzed.

Fig. 2 also shows that the normalized conditioned rates are increased with increasing $u'/S_L$ and $Ka$ (with the exception of a zone of $c_F > 0.9$ at $\phi$=0.5). While this effect is weakly pronounced in the plots, it is worth remembering that the rates are presented on a logarithmic scale. The reported profiles demonstrate that the magnitude of differential diffusion effects does not decrease (at least) on the local level in the studied range of $Ka$.

Fig. 3 presents profiles of (a)-(b) time-averaged conditioned temperature $\langle T|c_F\rangle(c_F)$ or (c)-(d) peak local temperature. These profiles are normalized using temperatures computed at the same $\phi$ and the same $c_F$ in unstretched laminar flames. Figs. 3(a) and 3(b) show that an increase in $u'/S_L$ and/or $Ka$ results in increasing the normalized $\langle T|c_F\rangle(c_F)$ at $c_F < 0.9$, but the effect is weakly pronounced in cases C, $\mathrm{C_{Ka}}$, and $\mathrm{C_{Da}}$. A similar trend is observed for $\max\{T(\mathbf{x},t)\}(c_F)$, see Figs. 3(c) and 3(d), with the effect being more (less) pronounced when compared to $\langle T|c_F\rangle(c_F)$ in cases C and $\mathrm{C_{Da}}$ or $\mathrm{C_{Ka}}$ (E and F, respectively).

For the goals of the present study, the following two trends are of the most importance; (i) the normalized temperatures are larger than unity (due to DDE, as discussed earlier[22,42,44]) and (ii) there is no sign that this effect is mitigated by turbulence if $c_F < 0.9$. Thus, on the local level, DDE result in significantly increasing not only FCR and HRR, as shown in Fig. 2, but also temperature in flame reaction zones.

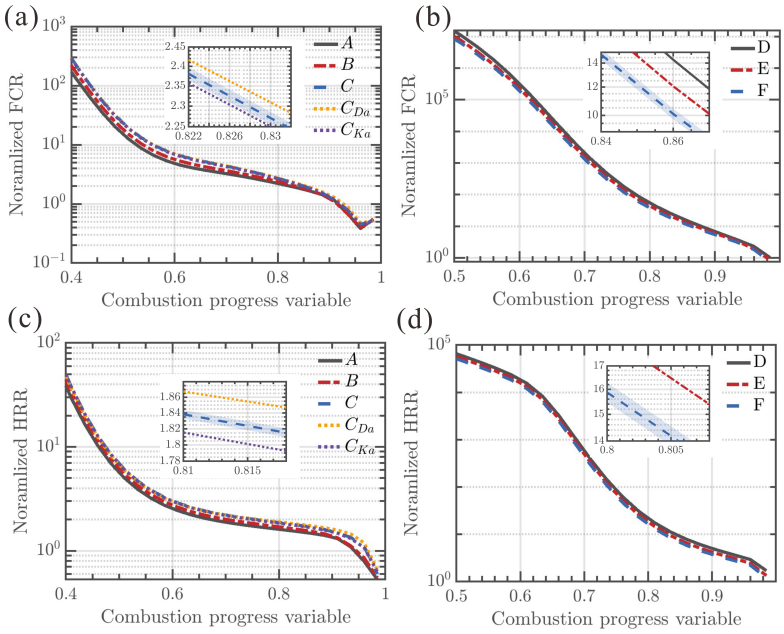


FIG. 2. Normalized time-averaged conditioned profiles of (a)-(b) FCR and (c)-(d) HRR. (a), (c) $\phi = 0.5$ and (b), (d) $\phi = 0.35$. Shaded regions illustrate the 95 % confidence intervals in a single representative case in each insert.

On the contrary, at large $c_F$, an increase in the local temperature is mitigated by turbulence. Indeed, (i) $\langle T|c_F\rangle(c_F \approx 0.95)$ is decreased with increasing $u'/S_L^0$ and $Ka$ in cases A-C, $C_{Ka}$, and $C_{Da}$, see Fig. 3(a), (ii) $\langle T|c_F\rangle(c_F \approx 0.97)$ is lowest in case D characterized by the largest $u'/S_L$ and $Ka$, see Fig. 3(b), (iii) $\max\{T(\mathbf{x},t)\}(c_F > 0.95)$ is lower in cases C and $C_{Da}$ when compared to cases A and B, see Fig. 3(c), and (iv) $\max\{T(\mathbf{x},t)\}(c_F > 0.9)$ is decreased with increasing $Ka$ from case F to case D, see Fig. 3(d). These trends are also observed in inserts in Fig. 3, where the same temperature profiles are re-normalized using $T_{ad}$ and are zoomed at large $c_F$. Inserts in Figs. 3(c) and 3(d) show that magnitude of super-adiabatic temperature decreases with increasing $Ka$ at $c_F$ close to unity.

It is worth emphasizing that the conditioned profiles presented in Figs. 2 and 3 converge well. For FCR and HRR, the good statistical convergence of the sampled data is shown by narrow shaded regions that illustrate the 95 % confidence intervals. To make Fig. 2

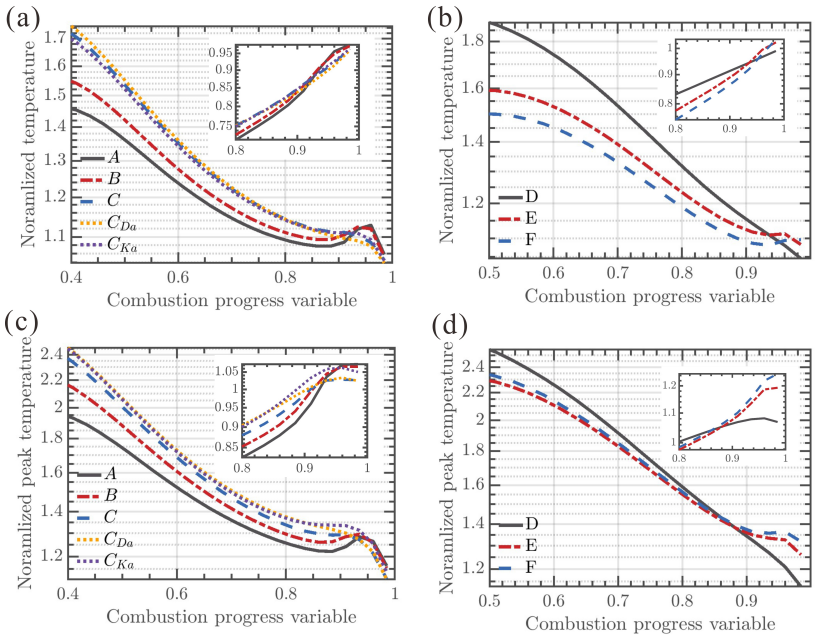


FIG. 3. Profiles of normalized (a)-(b) time-averaged conditioned temperature or (c)-(d) peak local temperature. (a), (c) $\phi = 0.5$ and (b), (d) $\phi = 0.35$. The same data re-normalized using $T_{ad}$ are zoomed in inserts.

readable, such shaded regions are plotted in a single representative case. In Fig. 4, such shaded regions are plotted for temperature profiles in all cases, but are highly zoomed to make the figures readable (the unzoomed temperature profiles without shaded regions are reported in Fig. 3). Finally, Fig. 5 shows maximum (over the studied interval of $c_F$) widths of the 95 % confidence intervals for normalized profiles of (a)-(b) $\langle \dot{\omega}_F | c_F \rangle (c_F)$ and $\langle \dot{\omega}_T | c_T \rangle (c_T)$ or (c)-(d) $\langle T | c_F \rangle (c_F)$ or $\max\{T(\mathbf{x}, t)\}(c_F)$. These maximum widths are very small for all profiles in richer flames ($\phi = 0.5$) and for the two temperatures in leaner flames ($\phi = 0.35$). Larger widths obtained for the rates (FCR and HRR) in the leaner flames stem from high values of $\langle \dot{\omega}_F | c_F \rangle (c_F)$ and $\langle \dot{\omega}_T | c_T \rangle (c_T)$ when compared to the peak rates $\max\{\dot{\omega}_{F,L}(c_F)\}$ and $\max\{\dot{\omega}_{T,L}(c_F)\}$ in the lean unstretched laminar flame. Since the latter peak rates are used to re-normalize the peak widths, the values reported in Fig. 5(d) are multiplied with a large ratio of $\langle \dot{\omega}_F | c_F \rangle / \max\{\dot{\omega}_{F,L}(c_F)\}$ or $\langle \dot{\omega}_T | c_F \rangle / \max\{\dot{\omega}_{T,L}(c_F)\}$.

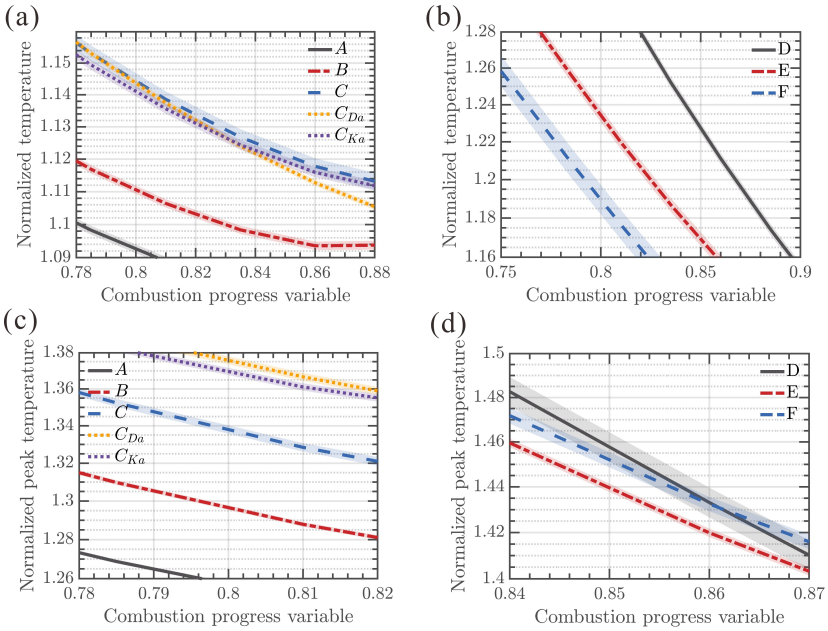


FIG. 4. Zoomed profiles of normalized (a)-(b) time-averaged conditioned temperature or (c)-(d) peak local temperature. (a), (c) $\phi = 0.5$ and (b), (d) $\phi = 0.35$. Shaded regions illustrate the 95 % confidence intervals.

Mitigation of the phenomenon of super-adiabatic temperature in lean $H_2$-air flames by turbulence is further indicated in Fig. 6. At large $c_F$, i.e., if $c_F > 0.95$ at $\phi$=0.5 or $c_F > 0.88$ at $\phi$=0.35, Figs. 6(a) and 6(b), respectively, show a decrease in the probability of finding super-adiabatic temperatures with increasing $u'/S_L$. Note that $c_F$-bin width is equal to 0.0001 and, hence, appearance of peak probabilities at $c_F$ close to unity is well resolved. It is also of interest to note that the reported conditioned probability is weakly affected by variations in $L/\delta_L$ at the same $u'/S_L$, cf. cases E and F in Fig. 6(b). This observation implies that appearance of hot spots characterized by $T(\mathbf{x}, t) > T_{ad}$ is a small-scale phenomenon, but further research into this issue is required.

As noted in the Introduction, mitigation of super-adiabatic temperature by turbulence was documented in earlier DNS[18,19,21,28,30] and experimental[35,36] studies. The novelty of the present analysis consists in stressing that this phenomenon does not prove mitigation of

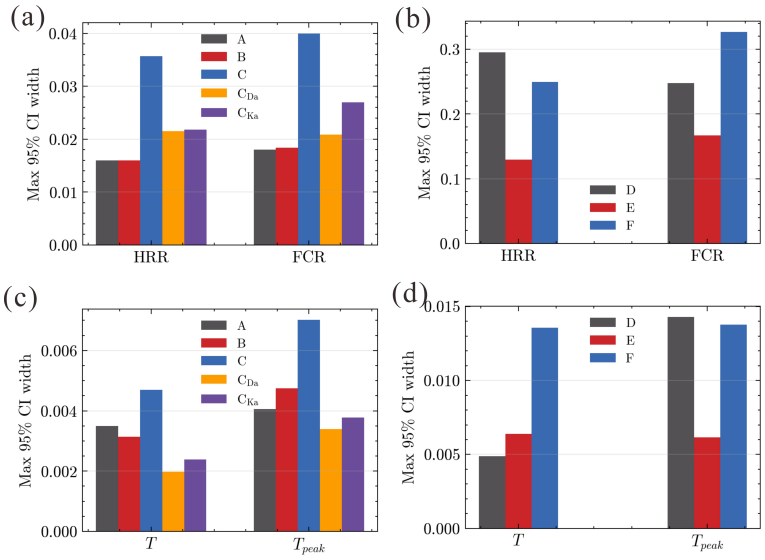


FIG. 5. Maximum (over the studied interval of $c_F$) widths of the 95 % confidence intervals for normalized (a)-(b) conditioned FCR and HRR or (c)-(d) conditioned and peak local temperatures. (a), (c) $\phi = 0.5$ and (b), (d) $\phi = 0.35$. The widths are re-normalized using the peak values of the considered quantities in unstretched laminar flames.

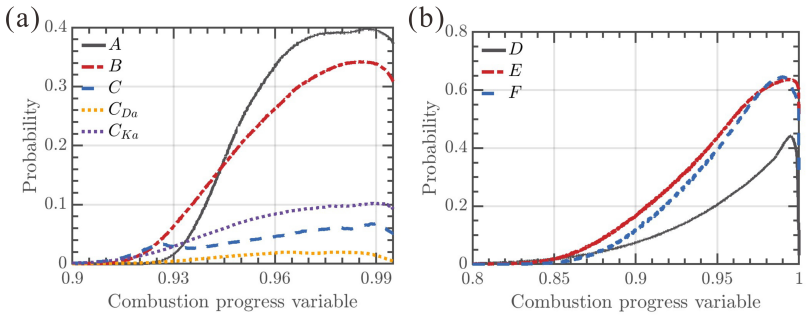


FIG. 6. Time-averaged conditioned probabilities of $T(\mathbf{x}, t) > T_{ad}$ in flames (a) A-C, $C_{Da}$ and $C_{Ka}$ or (b) D-F.

DDE by turbulence. On the contrary, in the analyzed cases, an increase in $Ka$ results not only in (i) reducing (i.a) the magnitude of super-adiabatic temperature, see Fig. 3, and (i.b) the probability a finding $T(\mathbf{x}, t) > T_{ad}$, see Fig. 6, but also in (ii) increasing both FCR and HRR within flame reaction zone, see Fig. 2.

These results are in line with a recent DNS study by Berger et al.[28] who have found that an increase in $Ka$ results in decreasing magnitude of super-adiabatic temperature but increasing a stretch factor,[37,60] which statistically quantifies an increase in burning rate due to DDE. Moreover, Fig. 3 in the paper by Berger et al.[28] indicates that the peak local HRR is weakly sensitive to variations in $Ka$. In the cited paper, these findings are not scrutinized but the increase in the stretch factor is attributed to "an increase of the mean equivalence ratio within the flame due to turbulent strain", see the abstract in the cited paper. However, this apparently plausible explanation (variations in $\phi$) does not allow for results of previous DNS studies[41,61] performed by (i) setting diffusivities of all species equal to the diffusivity of $H_2$ to suppress preferential diffusion effects by retaining a low $Le$ or (ii) setting the heat diffusivity of the mixture equal to $D_{H_2}$ to retain preferential diffusion at $Le$=1. Those DNS data clearly show that high burning rates documented in lean hydrogen-air turbulent flames are controlled by Lewis number, rather than variations in the local equivalence ratio due to preferential diffusion of $H_2$. Therefore, the opposite effects of turbulence on super-adiabatic temperature and on $U_T$, FCR, or HRR require further analyses and alternative approaches are worth considering.

The highlighted opposite effects of an increase in $Ka$ on (i) FCR and (ii) super-adiabatic temperature are associated with the fact that the FCR and temperature reach peak values in different local flame zones. Indeed, a typical complex-chemistry laminar flame is well known to involve a preheat zone, an inner layer, and an oxidation layer,[62,63] with (i) FCR being controlled by processes localized to the inner layer whereas (ii) the highest $T$ being reached in the oxidation zone. In this zone, the temperature grows due to heat release in slow termolecular radical recombination reactions, but the local HRR is significantly lower than its peak value and the local FCR almost vanishes. Therefore, processes localized to an oxidation layer substantially affect temperature field, contribute to heat release, and do not affect FCR, which is controlled by processes localized to the inner layer.

Thus, when a fluid volume with the local enthalpy excess (arisen due to DDE in highly curved and strained inner layers) moves through the oxidation layer, the volume temper-

ature (i) is increased due to heat release in termolecular recombination reactions, but (ii) is decreased due to small-scale turbulent mixing with surrounding volumes that have been weaker affected by DDE and are characterized by a lower $T$. At small or moderate $u'/S_L$ or $Ka$, the former process dominates, the local temperature continues growing and exceeds $T_{ad}$. In other words, small-scale turbulent mixing is too weak to smooth out hot spots originating due to DDE within highly curved and strained inner layers. When $u'/S_L$ and $Ka$ are increased, the local turbulent mixing is intensified within the oxidation layer and impedes appearing of super-adiabatic temperatures. At higher $Ka$, the turbulent mixing is expected to overwhelm the local heat release, and the local temperature remains lower than $T_{ad}$ even if DDE are well-pronounced at smaller $c_F(\mathbf{x}, t)$.

This physical scenario admits both (i) a significant increase in FCR, HRR, and, hence, $U_T/S_L$ due to the influence of DDE on the local inner-layer structure and (ii) disappearance of super-adiabatic temperatures at high $Ka$ due to small-scale turbulent mixing within oxidation layers. Thus, this scenario explains the opposite effects highlighted. It is consistent with Fig. 6, which shows a decrease in the probability of finding super-adiabatic temperatures with increasing $c_F$ at $c_F > c_F^* \approx 1$. Indeed, in a hypothetical adiabatic, no-mixing case, (i) $T(c_F)$ would be a monotonically increasing function due to termolecular radical recombination reactions with weak heat release and, hence, (ii) probability of $T(c_F) > T_{ad}$ could not decrease with increasing $c_F$. Therefore, the reported decrease in that probability with increasing $c_F$ is attributed to an important role played by mixing at $c_F^* < c_F < 1$, i.e., in the local flame oxidation zones. Specifically, mixing of hot spots (originating from DDE in the upstream local flame zones) with surrounding products could result in decreasing the local temperature in the hot spots provided that the surrounding products are characterized by a lower temperature, because they have less been affected by DDE. In such a case, the probability of $T(c_F) > T_{ad}$ could decrease with increasing $c_F$ at $c_F > c_F^*$. Recall that (i) $c_F^*$ varies from 0.9842 (case $\mathrm{C_{Da}}$) to 0.9948 (case D) and (ii) the bin width is equal to 0.0001. Therefore, appearance of peak probabilities at $c_F = c_F^*$ is a well-resolved phenomenon in the present study.

Fig. 7 further supports the discussed hypothesis by presenting typical images of hot spots, i.e., volumes where $T(\mathbf{x}, t) > 1.015 T_{ad}$ (the threshold 1.015 was selected to improve the image clarity). First, at lower $u'/S_L$, hot-spot volumes are significantly larger, cf. Figs. 7(a) and 7(c) or time-averaged probabilities of finding $T(\mathbf{x}, t) > 1.015 T_{ad}$, which are equal

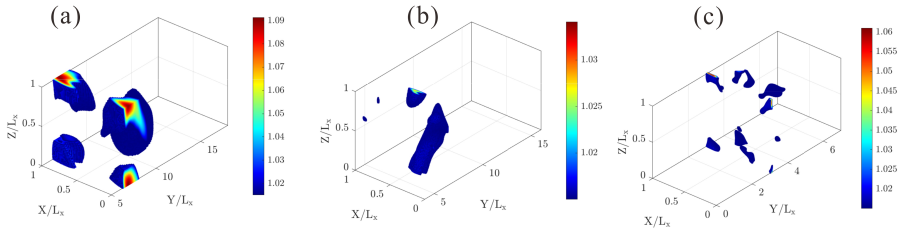


FIG. 7. Typical instantaneous images of hot spots, i.e., volumes where $T(\mathbf{x},t) > 1.015T_{ad}$, in flames (a) A, (b) C, and (c) $C_{Da}$. Color scales show $T(\mathbf{x},t)/T_{ad}$.

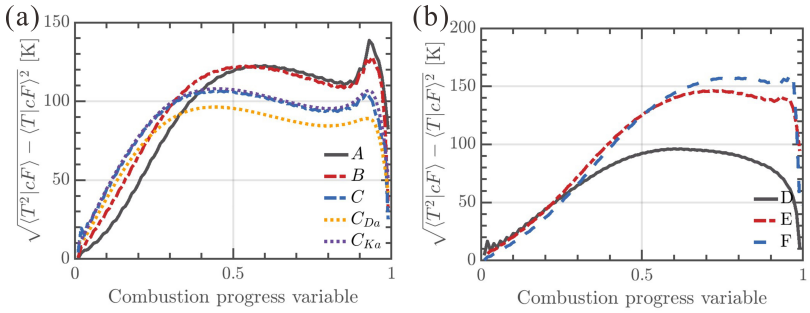


FIG. 8. Profiles of time-averaged rms conditioned temperature in flames (a) A-C, $C_{Da}$ and $C_{Ka}$ or (b) D-F.

to 0.03 and 0.0006 in cases A and $C_{Da}$, respectively. This observation is consistent with the emphasized smoothing effect of turbulent mixing on hot spots in the local flame oxidation zones. Second, in line with the smoothing effect of turbulent mixing, hot spots disappear at large distances from the mean flame front.

Finally, the discussed hypothesis is also supported in Figs. 8 and 9. Specifically, profiles of dimensional rms conditioned temperature, plotted in Fig. 8, show that $\sqrt{\langle T^2|c_F\rangle - \langle T|c_F\rangle^2}$ decreases with increasing $Ka$ at $c_F > 0.6$, thus, indicating more uniform, i.e., better mixed, temperature fields. This trend is associated with intensification of turbulent mixing at higher $Ka$. Nevertheless, if $c_F < 0.9$, such intensification of mixing does not suppress an increase in $\langle T|c_F\rangle$ due to DDE, see Fig. 3.

Fig. 9(a) reports the time- and transverse-averaged contributions $\chi^* = \langle \chi H(c_F - c_F^*)\rangle$ of the trailing zone of instantaneous flame (or oxidation layer in other words), computed using

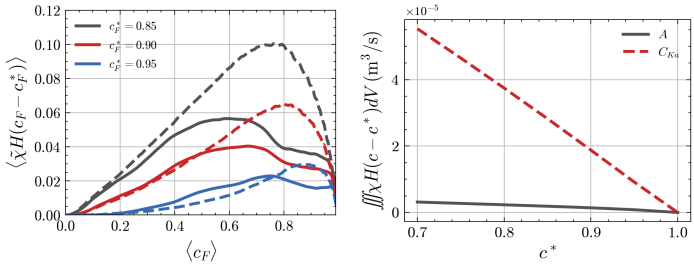


(a) (b)

FIG. 9. Time- and transverse-averaged scalar dissipation rate $\chi^* = \langle \chi H(c_F - c_F^*) \rangle$ vs. $(a)$ time- and transverse-averaged $\langle c_F \rangle$ or $(b)$ threshold $c_F^*$. Solid and dashed lines show the rates computed in flames A and $C_{Ka}$, respectively. $(a)$ Results are normalized using flame time scale $\tau_F$ and shown for three different $c_F^*$ specified in legends. $(b)$ Dimensional results sampled from the entire flame brush.

three different threshold values $c_F^*$, specified in the figure, to the scalar dissipation rate. At large $\langle c_F \rangle$, i.e., in the trailing zone of turbulent flame brush, this contribution is significantly larger in highly turbulent flame $C_{Ka}$ when compared to weakly turbulent flame A, cf. curves plotted in dashed and solid lines, respectively. Here, $\chi = \lambda/[\rho c_p (T_{ad} - T_u)^2] \nabla T \cdot \nabla T$ is scalar dissipation rate, $\lambda$ is molecular heat conductivity, $c_p$ is heat capacity, $H$ designates Heaviside function, and $\langle c_F \rangle$ is time- and transverse-averaged value of combustion progress variable. The same trend is well observed in Fig. 9(b), which reports $\chi^*$ sampled from the entire flame brush vs. the threshold value $c^*$.

## IV. CONCLUDING REMARKS

The performed analyses of DNS data obtained from eight complex-chemistry lean $H_2$-air turbulent flames show that, at sufficiently high $Ka$, (i) both magnitude of super-adiabatic temperature and probability of finding it are decreased with increasing Karlovitz number, whereas (ii) significant influence of differential diffusion effects on the local structure of flame reaction zones and burning rate is not mitigated by turbulence in all cases, even at $Ka$ as high as 1315. Thus, the two phenomena (super-adiabatic hot spots and an increase in burning rate due to differential diffusion effects) are not inextricably linked. Differential

diffusion can increase local burning rate in the inner layer even if turbulence is intense enough to suppress the appearance of super-adiabatic hot spots. Therefore, a decrease in the magnitude of super-adiabatic local temperature with increasing Karlovitz number or even negligible probability of finding such a high temperature at high $Ka$ does not prove that differential diffusion effects play a minor role.

Under conditions of this study, the aforementioned reduction of super-adiabatic temperature is attributed to turbulent mixing in local flame oxidation zones, rather than weakening differential diffusion effects in local flame reaction zones.

## V. ACKNOWLEDGMENTS

ANL gratefully acknowledges the financial support by Swedish Research Council (Grant No. 2023-04407). Chinese authors have been supported in part by NSFC (Grant Nos. 12225204 and 51976088), the Shenzhen Science and Technology Program (Grant No. SYSPG20241211173725008 and JCYJ20210324104802005), Department of Science and Technology of Guangdong Province (Grant No. 2023B1212060001 and 2020B1212030001), and the Center for Computational Science and Engineering of Southern University of Science and Technology.

## REFERENCES

[1]V. R. Kuznetsov and V. A. Sabelnikov, *Turbulence and Combustion* (Hemisphere New York, 1990).

[2]A. N. Lipatnikov and J. Chomiak, "Molecular transport effects on turbulent flame propagation and structure," Prog. Energy Combust. Sci. **31**, 1–73 (2005).

[3]S. Hochgreb, "How fast can we burn, 2.0," Proc. Combust. Inst. **39**, 2077–2105 (2023).

[4]H. Pitsch, "The transition to sustainable combustion: Hydrogen- and carbon-based future fuels and methods for dealing with their challenges," Proc. Combust. Inst. **40**, 105638 (2024).

[5]Y. Zel'dovich, *Theory of Combustion and Gas Detonation* (Akad. Nauk SSSR, 1944).

[6]F. A. Williams, *Combustion Theory* (CRC Press, 1985).

[7]V. P. Karpov and A. S. Sokolik, "Inflammation limits in turbulized gas mixtures," Proc. Acad. Sci. USSR, Phys. Chem. **141**, 866–869 (1961).

[8]V. P. Karpov and E. S. Severin, "Effects of molecular-transport coefficients on the rate of turbulent combustion," Combust. Explos. Shock Waves **16**, 41–46 (1980).

[9]M. S. Wu, A. Kwon, G. Driscoll, and G. M. Faeth, "Turbulent premixed hydrogen/air flames at high Reynolds numbers," Combust. Sci. and Technol. **73**, 327–350 (1990).

[10]P. Venkateswaran, A. Marshall, J. Seitzman, and T. Lieuwen, "Pressure and fuel effects on turbulent consumption speeds of $H_2$/CO blends," Proc. Combust. Inst. **34**, 1527–1535 (2013).

[11]S. Yang, A. Saha, W. Liang, and C. K. Law, "Extreme role of preferential diffusion in turbulent flame propagation," Combust. Flame **188**, 498–504 (2018).

[12]X. Cai, Q. Fan, X. S. Bai, J. Wang, M. Zhang, Z. Huang, M. Aldén, and Z. Li, "Turbulent burning velocity and its related statistics of ammonia-hydrogen-air jet flames at high Karlovitz number: Effect of differential diffusion," Proc. Combust. Inst. **39**, 4215–4226 (2023).

[13]A. N. Lipatnikov, Y. R. Chen, and S. S. Shy, "An experimental study of the influence of Lewis number on turbulent flame speed at different pressures," Proc. Combust. Inst. **39**, 2339–2347 (2023).

[14]S. Wang, A. M. Elbaz, Z. Wang, and W. L. Roberts, "Turbulent flame speed measurement of $NH_3/H_2$/air and $CH_4$/air flames and a numerical case study of NO emission in a constant volume combustion chamber (C.V.C.C.)," Fuel **332**, 126152 (2023).

[15]H. Y. Hsieh, S. M. Mousavi, A. N. Lipatnikov, and S. S. Shy, "Experimental study of the influence of Lewis number, laminar flame thickness, temperature, and pressure on turbulent flame speed using hydrogen and methane fuels," Proc. Combust. Inst. **40**, 105752 (2024).

[16]Z. Wang, X. Li, T. Li, A. Dreizler, S. M. Mousavi, A. N. Lipatnikov, and B. Zhou, "Experimental investigation of $NH_3/H_2$ jet flames adopting multi-scalar imaging: Comparison of turbulent burning velocities obtained using different flame-front markers," Combust. Flame **275**, 114054 (2025).

[17]M. S. Day, J. B. Bell, V. Bremer, V. E. Pascucci, V. E. Beckner, and M. J. Lijewski, "Turbulence effects on cellular burning structures in lean premixed hydrogen flames," Combust. Flame **156**, 1035–1045 (2009).

[18]A. J. Aspden, M. S. Day, and J. B. Bell, "Turbulence-flame interactions in lean premixed hydrogen: transition to the distributed burning regime," J. Fluid Mech. **680**, 287–320 (2011).

[19]B. Savard and G. Blanquart, "An a priori model for the effective species Lewis numbers in premixed turbulent flames," Combust. Flame **161**, 1547–1557 (2014).

[20]X. Wang, T. Jin, and K. H. Luo, "Response of heat release to equivalence ratio variations in high Karlovitz premixed $H_2$/air flames at 20 atm," Int. J. Hydrogen Energy **44**, 3195–3207 (2019).

[21]A. J. Aspden, M. S. Day, and J. B. Bell, "Towards the distributed burning regime in turbulent premixed flames," J. Fluid Mech. **871**, 1–21 (2019).

[22]H. C. Lee, P. Dai, M. Wan, and A. N. Lipatnikov, "Influence of molecular transport on burning rate and conditioned species concentrations in highly turbulent premixed flames," J. Fluid Mech. **928**, A5 (2021).

[23]L. Berger, A. Attili, and H. Pitsch, "Synergistic interactions of thermodiffusive instabilities and turbulence in lean hydrogen flames," Combust. Flame **244**, 112254 (2022).

[24]M. Rieth, A. Gruber, F. A. Williams, and J. H. Chen, "Enhanced burning rates in hydrogen-enriched turbulent premixed flames by diffusion of molecular and atomic hydrogen," Combust. Flame **239**, 111740 (2022).

[25]M. Rieth, A. Gruber, and J. H. Chen, "The effect of pressure on lean premixed hydrogen-air flames," Combust. Flame **250**, 112514 (2023).

[26]T. L. Howarth, E. F. Hunt, and A. J. Aspden, "Thermodiffusively-unstable lean premixed hydrogen flames: Phenomenology, empirical modelling, and thermal leading points," Combust. Flame **256**, 112811 (2023).

[27]V. Coulon, J. Gaucherand, V. Xing, D. Laera, C. Lapeyre, and T. Poinsot, "Direct numerical simulations of methane, ammonia-hydrogen and hydrogen turbulent premixed flames," Combust. Flame **256**, 112933 (2023).

[28]L. Berger, A. Attili, M. Gauding, and H. Pitsch, "Effects of Karlovitz number variations on thermodiffusive instabilities in lean turbulent hydrogen jet flames," Proc. Combust. Inst. **40**, 105219 (2024).

[29]H. Böttler, D. Kaddar, T. J. P. Karpowski, F. Ferraro, A. Scholtissek, H. Nicolai, and C. Hasse, "Can flamelet manifolds capture the interactions of thermo-diffusive instabilities and turbulence in lean hydrogen flames? - an apriori analysis," Int. J. Hydrogen Energy

**56**, 1397–1407 (2024).

[30]M. X. Yao and G. Blanquart, "Isolating effects of large and small scale turbulence on thermodiffusively unstable premixed hydrogen flames," Combust. Flame **269**, 113657 (2024).

[31]Y. Wang, C. Xu, C. Chi, Y. Yang, and Z. Chen, "Temperature effect on turbulent burning velocity of lean premixed hydrogen/air flames," Phys. Fluids **36**, 125165 (2024).

[32]F. A. Meziat Ramirez, Q. Douasbin, O. Dounia, O. Vermorel, and T. Jaravel, "Flame-turbulence interactions in lean hydrogen flames: Implications for turbulent flame speed and fractal modelling," Combust. Flame **273**, 113926 (2025).

[33]Y. Wang, C. Xu, and R. Scarcelli, "Turbulent burning velocity of lean premixed hydrogen/air flames at engine conditions: Effects of turbulence intensity and length scale," Combust. Flame **282**, 114504 (2025).

[34]V. S. Wehrmann, N. Chakraborty, M. Klein, and J. Hasslberger, "On local equivalence ratio dependence of the burning rate in premixed turbulent lean hydrogen/air flames: A direct numerical simulation analysis," Flow Turbul. Combust. **116**, 19 (2026).

[35]S. Shi, R. Schultheis, R. S. Barlow, D. Geyer, D. Dreizler, and T. Li, "Internal flame structures of thermo-diffusive lean premixed $H_2$/air flames with increasing turbulence," Proc. Combust. Inst. **40**, 105225 (2024).

[36]S. Shi, R. Schultheis, R. S. Barlow, D. Geyer, D. Dreizler, and T. Li, "Assessing turbulence-flame interaction of thermo-diffusive lean premixed $H_2$/air flames towards distributed burning regime," Combust. Flame **269**, 113699 (2024).

[37]D. Bradley, A. K. C. Lau, and M. Lawes, "Flame stretch rate as a determinant of turbulent burning velocity," Phil. Trans. R. Soc. London A **338**, 359–387 (1992).

[38]A. N. Lipatnikov, *Fundamentals of Premixed Turbulent Combustion* (CRC Press, 2012).

[39]H. C. Lee, P. Dai, M. Wan, and A. N. Lipatnikov, "A DNS study of extreme and leading points in lean hydrogen-air turbulent flames - part I: Local thermochemical structure and reaction rates," Combust. Flame **235**, 111716 (2022).

[40]H. C. Lee, P. Dai, M. Wan, and A. N. Lipatnikov, "A DNS study of extreme and leading points in lean hydrogen-air turbulent flames - part II: Local velocity field and flame topology," Combust. Flame **235**, 111712 (2022).

[41]H. C. Lee, P. Dai, M. Wan, and A. N. Lipatnikov, "Lewis number and preferential diffusion effects in lean hydrogen–air highly turbulent flames," Phys. Fluids **34**, 035131 (2022).

[42]H. C. Lee, P. Dai, M. Wan, and A. N. Lipatnikov, "A numerical support of leading point concept," Int. J. Hydrogen Energy **47**, 23444–23461 (2022).

[43]H. C. Lee, A. Abdelsamie, P. Dai, M. Wan, and A. N. Lipatnikov, "Influence of equivalence ratio on turbulent burning velocity and extreme fuel consumption rate in lean hydrogen-air turbulent flames," Fuel **327**, 124969 (2022).

[44]H. C. Lee, P. Dai, M. Wan, and A. N. Lipatnikov, "Displacement speed, flame surface density, and burning rate in highly turbulent premixed flames characterized by low Lewis numbers," J. Fluid Mech. **961**, A21 (2023).

[45]H. C. Lee, B. Wu, P. Dai, M. Wan, and A. N. Lipatnikov, "Area increase and stretch factor in lean hydrogen-air turbulent flames," Proc. Combust. Inst. **40**, 105687 (2024).

[46]H. C. Lee, B. Wu, P. Dai, M. Wan, and A. N. Lipatnikov, "Comparison of characteristics of unstable laminar and turbulent lean hydrogen–air flames," Phys. Fluids **37**, 085182 (2025).

[47]X. Guan, H. C. Lee, P. Dai, M. Wan, and A. N. Lipatnikov, "Morphology of instantaneous flame surfaces in laminar and turbulent lean $H_2$-air flames," Int. J. Hydrogen Energy **189**, 152110 (2025).

[48]A. Abdelsamie, G. Fru, T. Oster, F. Dietzsch, G. Janiga, and D. Thévenin, "Towards direct numerical simulations of low-Mach number turbulent reacting and two-phase flows using immersed boundaries," Comput. Fluids **131**, 123–141 (2016).

[49]A. Kéromnès, W. K. Metcalfe, K. A. Heufer, N. Donohoe, A. K. Das, C. J. Sung, J. Herzler, C. Naumann, P. Griebel, O. Mathieu, M. C. Krejci, E. J. Petersen, W. J. Pitz, and H. J. Curran, "An experimental and detailed chemical kinetic modeling study of hydrogen and syngas mixture oxidation at elevated pressures," Combust. Flame **160**, 995–1011 (2013).

[50]D. Goodwin, N. Malaya, H. Moffat, and R. Speth, "Cantera: An object-oriented software toolkit for chemical kinetics, thermodynamics, and transport processes," Caltech, Pasadena, CA (2009).

[51]J. F. Grcar, J. B. Bell, and M. S. Day, "The Soret effect in naturally propagating, premixed, lean, hydrogen-air flames," Proc. Combust. Inst. **32**, 1173–1180 (2009).

[52]P. Domingo and L. Vervisch, "Recent developments in DNS of turbulent combustion," Proc. Combust. Inst. **39**, 2055–2076 (2023).

[53]B. Bobbitt, S. Lapointe, and G. Blanquart, "Vorticity transformation in high Karlovitz number premixed flames," Phys. Fluids **28**, 015101 (2016).

[54]B. Bobbitt and G. Blanquart, "Vorticity isotropy in high Karlovitz number premixed flames," Phys. Fluids **28**, 105101 (2016).

[55]A. N. Lipatnikov and J. Chomiak, "Turbulent flame speed and thickness: phenomenology, evaluation, and application in multi-dimensional simulations," Prog. Energy Combust. Sci. **28**, 1–74 (2002).

[56]R. Yu and A. N. Lipatnikov, "DNS study of dependence of bulk consumption velocity in a constant-density reacting flow on turbulence and mixture characteristics," Phys. Fluids **29**, 065116 (2017).

[57]A. N. Lipatnikov, V. A. Sabelnikov, F. E. Hernández-Pérez, W. Song, and H. G. Im, "A priori DNS study of applicability of flamelet concept to predicting mean concentrations of species in turbulent premixed flames at various Karlovitz numbers," Combust. Flame **222**, 370–382 (2020).

[58]A. R. Varma, U. Ahmed, K. Klein, and N. Chakraborty, "Effects of turbulent length scale on the bending effect of turbulent burning velocity in premixed turbulent combustion," Combust. Flame **233**, 111569 (2021).

[59]W. Song, F. E. Hernández-Pérez, E. A. Tingas, and H. G. Im, "Statistics of local and global flame speed and structure for highly turbulent $H_2$/air premixed flames," Combust. Flame **232**, 111523 (2021).

[60]K. N. C. Bray and R. S. Cant, "Some applications of Kolmogorov's turbulence research in the field of combustion," Proc. R. Soc. London A **434**, 217–240 (1991).

[61]A. J. Aspden, "A numerical study of diffusive effects in turbulent lean premixed hydrogen flames," Proc. Combust. Inst. **36**, 1997–2004 (2017).

[62]F. A. Williams, "Progress in knowledge of flamelet structure and extinction," Prog. Energy Combust. Sci. **26**, 657–682 (2000).

[63]J. Buckmaster, P. Clavin, A. Liñan, M. Matalon, N. Peters, G. Sivashinsky, and F. A. Williams, "Combustion theory and modeling," Proc. Combust. Inst. **30**, 1–19 (2005).